Evaluation of the structural-phase characteristics of a supersaturated ultrafine-grained Au-Co solid solution by diffractometry in hard synchrotron radiation

Cite as: AIP Conference Proceedings **2299**, 040003 (2020); https://doi.org/10.1063/5.0031132
Published Online: 17 November 2020

T. P. Tolmachev, V. P. Pilyugin, A. I. Ancharov, A. M. Patselov, E. G. Chernyshev, and Yu.V. Solov'eva

Evaluation of the Structural-Phase Characteristics of a Supersaturated Ultrafine-Grained Au-Co Solid Solution by Diffractometry in Hard Synchrotron Radiation

T.P. Tolmachev [1, 2, 3 a)], V.P. Pilyugin[2, 3, b)], A.I. Ancharov[4,5,6, c)], A.M. Patselov[2, d)], E.G. Chernyshev [2, e)] and Yu.V. Solov'eva[7, f)]

[1]*Institute of Engineering Science, Ural Branch of the Russian Academy of Sciences, 34 Komsomolskaya st., 620049, Ekaterinburg, Russia*
[2]*M.N. Miheev Institute of Metal Physics of Ural Branch of Russian Academy of Sciences, 18 S. Kovalevskaya Street, Yekaterinburg, Russian Federation, 620108*
[3]*Ural Federal University, 620002, 19 Mira street, Ekaterinburg, Russia*
[4]*Institute of Solid State Chemistry and Mechanochemistry of the Siberian Branch of the Russian Academy of Sciences, Kutateladze 18, 630128 Novosibirsk, Russia*
[5]*Budker Institute of Nuclear Physics of Siberian Branch Russian Academy of Sciences, 11, Acad. Lavrentieva Pr., Novosibirsk, 630090, Russia*
[6]*Novosibirsk State University, 1, Pirogova str., Novosibirsk, 630090, Russia*
[7]*Tomsk State University of Architecture and Building, 2, pl. Solyanaya, Tomsk, 634003, Russia*

[a)]Corresponding author: tolmachev@imp.uran.ru
[b)]pilyugin@ imp.uran.ru
[c)]ancharov@mail.ru
[d)]patselov@imp.uran.ru
[e)]eucher@imp.uran.ru
[f)]j_sol@mail.ru

Abstract. A synchrotron radiation study of immiscible Au-Co alloys obtained by consolidating a heterogeneous mixture of components and subsequent severe plastic deformation was performed. Namely, the estimates of the crystal lattice parameter, the average size of the coherent scattering regions and lattice strains in mechanically alloyed supersaturated solid solutions were made using obtained diffraction patterns and diffraction spectra. The effect of the temperature regime of deformation processing on the listed characteristics is shown, when the transition from cold deformation to cryogenic is carried out.

INTRODUCTION

The directed formation of the structure and properties of alloys from immiscible ferromagnetic and non-ferromagnetic components is being intensively studied due to the high potential of their application [1, 2]. Obtaining a supersaturated solid solution can be the basis for such regulation of the state of the alloy.

Mechanical alloying by severe plastic deformation makes it possible to obtain ultrafine-grained (submicro- and nanocrystalline) alloys with the formation of metastable phases [3] including supersaturated solid solutions.

The Au-Co system is characterized by the limited solubility of the components [4] and by the difference in their structural and physical-mechanical characteristics. The enthalpy of mixing is +34 kJ/mol [5]. Supersaturated Au-Co solid solutions were obtained in the form of thin films, coatings, or particles using the appropriate nonequilibrium

Synchrotron and Free Electron Laser Radiation
AIP Conf. Proc. 2299, 040003-1–040003-7; https://doi.org/10.1063/5.0031132
Published by AIP Publishing. 978-0-7354-4033-3/$30.00

methods [6-8]. In this work, the Au-Co alloy was obtained in bulk nanocrystalline form, which is suitable for further study without additional thermo mechanical action.

To achieve the state of a homogeneous solid solution, it is necessary to use the possibility of realizing severe plastic deformations, as well as changing the mechanisms of formation of structures and phases through changing processing parameters. This parameter can be a different temperature regime, for example, deformation under cryogenic temperatures, as in present paper. To take into account possible inhomogeneities in the strain distribution, it is necessary to localize the area of structural-phase studies. In addition, it is necessary to obtain data on the state not only on the surface, but also in the bulk of the alloy. In this work, synchrotron radiation with a short X-ray wavelength was used due to its advantages for such tasks, due to its high penetrating power and the possibility of obtaining the entire diffraction pattern.

EXPERIMENTAL

Cobalt and gold in the initial state were powders with a particle size of about 50 μm and 300 μm, respectively. The purity of the components was 99.60% and 99.99%, respectively. Powders of these metals were mixed in an equiatomic ratio.

Next, the powder mixtures were processed by shear deformation under high quasi-hydrostatic pressure (so called "high-pressure torsion", HPT) on Bridgman anvils [9-11]. The type of anvils is "quasi constrained" with a diameter of 5 mm. The material of the anvils is a super hard alloy WC6 with a hardness of 92 HRC.

The processing pressure was 8 GPa, which is sufficient to plasticize the components upon deformation. The alloy samples had a disk shape with a diameter of about 5 mm and a thickness of about 0.1 mm after processing. The rotation speed of the anvils was 1 rpm.

To reduce the inhomogeneity of the deformation along the radius of the disk samples, the reprocessing technique was used, which consisted in the following. After 10 turns at one stage of processing, the sample in a disk shape is cut into sectors, and then these parts are put back into a processing cell. The number of reprocessing stages was 3, i.e. the total number of anvil revolutions was 30.

HPT was carried out under two temperature conditions: cold (at room temperature) and cryogenic (at the temperature of boiling liquid nitrogen) deformation.

X-ray study was carried out using a hard X-ray wavelength of 0.03685 nm and transmission geometry mode at the station of the 4th synchrotron radiation channel of the VEPP-3 accelerator of the Siberian Synchrotron and Terahertz Radiation Center, Budker Institute of Nuclear Physics [12-14] at room temperature. Two-dimensional diffraction patterns were recorded by a mar345 two-coordinate detector. A more detailed description of the SR XRD analysis can be found elsewhere [12, 13, 15, 16].

RESULTS AND DISCUSSION

The number of revolutions of the anvil was 30 taking into account the redistribution procedure. It is necessary to use the formula [17] to estimate the true strain:

$$e = \ln\left(1 + \left(\frac{\varphi R}{h_k}\right)^2\right)^{0.5} \quad (1)$$

where φ is the angle of rotation of the anvil in radians, R is the distance from the center of the sample, h_k is the thickness of the sample, and e is the true shear strain.

Since the initial state was in the form of a bulk powder, the deformation upon upsetting formula was not used. The central and peripheral parts of the sample periodically change places in the working cell during the reprocessing procedure. Therefore, getting true strain for the center and periphery seems to be incorrect. Instead, the calculation was performed at half the radius of the sample. In this case, the deformation value was 8.1. Thus, this process is characterized by a high enough value of severe plastic deformation.

As a result of transmission synchrotron diffraction, X-ray diffraction patterns were obtained from the central and peripheral regions of the alloy samples (Fig.1). Based on the shape of the lines in the form of Debye rings, taking into account the true strain, and also taking into account the wavelength of the radiation used, it can be assumed that

an ultrafine-grained state is formed in the alloy sample. It can be seen from the mutual arrangement of the reflections that a state is formed in the alloy samples in the form of a phase with an fcc lattice. The presence of a phase associated with the low-temperature modification of cobalt was not observed according to X-ray diffraction data.

The presence of texture after deformation processing was noted, with the most intense texture maxima present in the X-ray diffraction patterns in the center (Fig. 1a) and especially at the edge of the disk (Fig. 1b) of the alloy sample obtained by cold deformation. In the X-ray diffraction patterns of alloys after cryogenic deformation, the texture maxima are significantly blurred, and their intensity is significantly inferior to those in the X-ray diffraction patterns of cryo-HPT alloys (Fig. 1c, d).

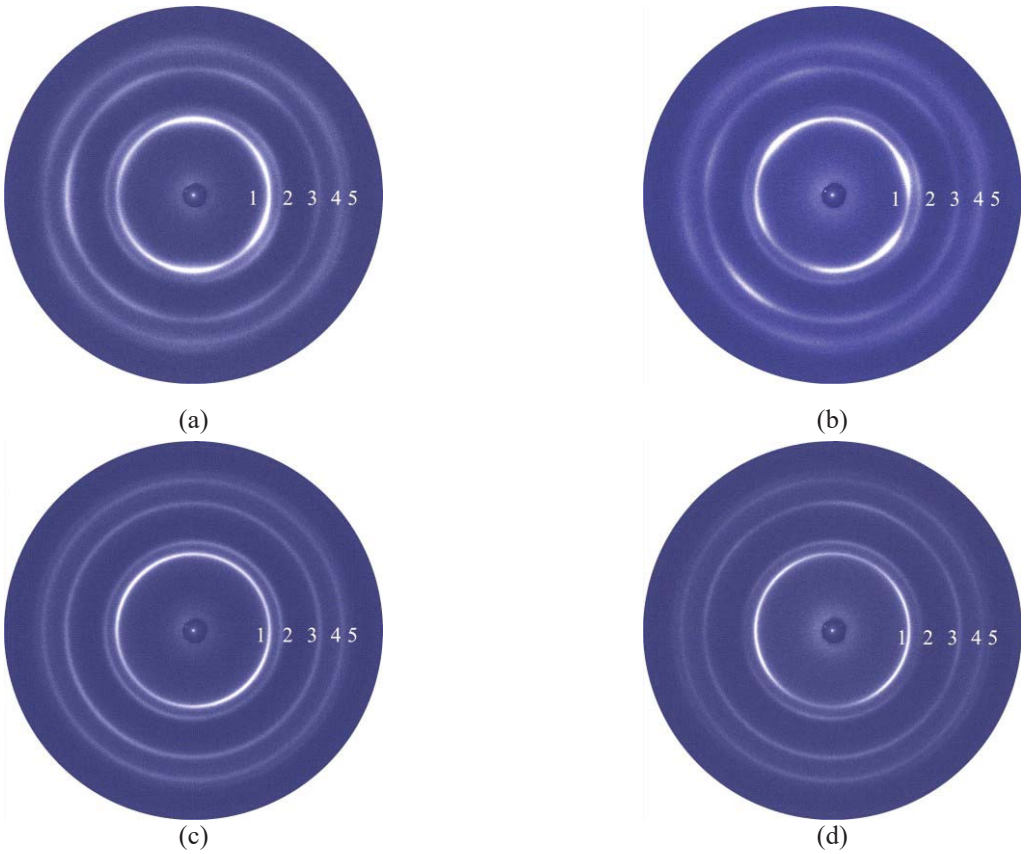

FIGURE 1. X-ray diffraction patterns in SI of Au-Co alloys obtained at room HPT in the center of the sample (a) and at the periphery (b); and cryo-HPC in the center of the sample (c) and at the periphery (d). The numbers indicate the serial number of the Debye ring from the central spot.

The thickness of the Debye rings in the X-ray diffraction patterns of alloys obtained by cryodeformation is, on average, less than in the X-ray patterns in the case of cold deformation.

Most part of the X-ray diffraction patterns were converted to diffraction spectra shown in Fig. 2.

The indexing of the Debye rings confirmed the formation of a phase with an fcc lattice as a result of HPT. From the values of the lattice parameter of the fcc phase in the X-ray diffraction patterns the ratio of the components in each phase was obtained. It was found that in all four cases the phases in the X-ray diffraction patterns refer to supersaturated fcc solid solutions of cobalt in a gold-based matrix. The diffraction spectra data were also used to calculate the lattice parameters of the fcc solid solution based on gold and to obtain the ratios of the components in it. Table 1 shows the correspondence of the lines and reflections on the X-ray diffraction patterns and spectra in order from the central spot to hkl planes with an interplanar spacings d. Those data that, with errors, were averaged over data from X-ray diffraction patterns and spectra, the rest are given only on the basis of X-ray patterns. Table 1 also shows lattice parameters and the proportions of cobalt of the supersaturated solid solutions.

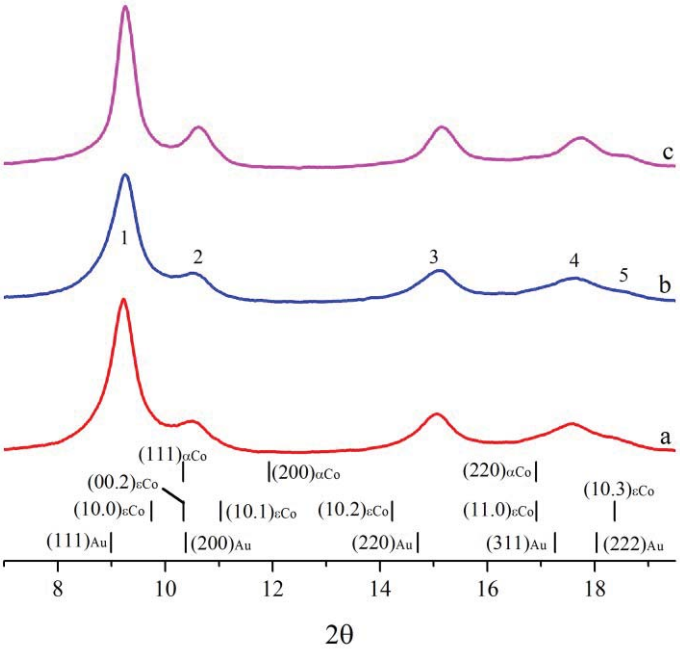

FIGURE 2. Diffraction spectra in SR of Au-Co alloys obtained at room HPT in the center of the sample (a) and at the periphery (b); and cryo-HPT in the center of the sample (c). The numbers show the serial number of the reflex with increasing diffraction angle.

TABLE 1. Data on interference indices, interplanar spacings, and lines of X-ray and diffraction spectra, as well as estimates of lattice parameters and compositions of supersaturated Au-Co solid solutions depending on the sample region and temperature regime of deformation.

Peak No.	*hkl*	Cold Worked Au-Co Alloy		Cryo-Deformed Au-Co Alloy	
		Sample Center	Sample Periphery	Sample Center	Sample Periphery
		***d*, nm**	***d*, nm**	***d*, nm**	***d*, nm**
1	111	0,2294±0,0024	0,2284±0,0050	0,2280±0,0014	0,2271
2	200	0,1999±0,0131	0,2012±0,0096	0,1981±0,0014	0,1949
3	220	0,1406±0,0013	0,1405±0,0001	0,1396±0,0009	0,1383
4	311	0,1205±0,0003	0,1203±0,0003	0,1191±0,0011	0,1181
5	222	0,1147	0,1139	0,1131	0,1130
Lattice parameter, nm		0,3985±0,0004	0,3982±0,0001	0,3949±0,0005	0,3914
Solid solution Au-X at. % Co		25±1	26,5±0,5	34±1	40

As can be seen, as a result of room HPT, approximately the same proportion of cobalt was dissolved in the gold-based matrix in the center and at the periphery of the sample. At the same time, as a result of cryo HPT, the solubility of cobalt increased, and in the center of the sample the increase in the proportion of cobalt was about 10 at. %, and at the periphery - about 15 at. %.

The data from diffraction spectra and from X-ray diffraction patterns differ by no more than 2 at. %, and the values of the interplanar spacings are in good agreement with each other, especially for the peaks (220) and (311). In addition, in the diffraction spectra, the width of the reflections is significant so that closely spaced peaks partially overlap each other. This indicates a significant dispersion of the structure after HPT-deformation. Also, from the diffraction spectra, we can speak of the presence of a phase associated with cobalt, the intensity of which is low relative to the phase based on gold.

Based on the level of mechanical dissolution of cobalt, it is worth noting that the above estimate of the true strain for the entire alloy specimen has a reason in the case of cold deformation, however, in the case of cryogenic deformation, the radial dependence of the true strain remains despite the reprocessing procedure.

To assess the dispersion of the structure based on the data of diffraction spectra, the coherent scattering regions and lattice strains were calculated using the Selyakov-Scherrer and Stokes-Wilson formulas, respectively:

$$D = \frac{0.9\lambda}{\beta \cos\theta}, \ \varepsilon = \frac{\beta}{4tg\theta} \tag{2}$$

where D is the coherent scattering region size in nm, ε is the lattice strain in arb. units, λ is the wavelength, β is the FWHM, θ is the diffraction angle. The data are presented in Table 2.

TABLE 2. Estimated values of the coherent scattering region size (D) and lattice strain (ε) in the center and at the periphery of alloy samples after room- and cryo-HPT.

hkl	**Cold Worked Alloy**				**Cryo-Deformed Alloy**	
	Sample Center		**Sample Periphery**		**Sample Center**	
	***D*, nm**	**ε * 10^{-2}**	***D*, nm**	**ε* 10^{-2}**	***D*, nm**	**ε* 10^{-2}**
111	2,8	3,7	2,5	4,1	5,1	2,0
200	2,5	3,7	1,8	5,0	3,5	2,5
220	2,3	2,8	2,2	2,9	2,7	2,4
311	1,3	4,0	1,4	3,8	1,6	3,4
average	2,2	3,6	2,0	4,0	3,2	2,6

It is seen that in different directions the linear dimensions of the coherent scattering regions and lattice strains are not the same. The similar character of the values indicates that, after deformation, the crystallites are oriented in a certain way, which leads to the formation of a shear deformation under pressure texture. On average, the dispersion after deformation at room temperature is greater than at cryogenic. The same is true for the average value of lattice strain.

CONCLUSIONS

As a result of mechanical alloying by severe plastic deformation by shear deformation under high pressure, alloys with a significant content of the phase of a supersaturated fcc solid substitutional solution Au-Co were formed (Table 3). The alloy obtained at room HPT is characterized by increased dispersion, the level of microstresses and the severity of texture in comparison with the alloy obtained by cryo HPT. In this case, as a result of mechanical alloying in both temperature regimes, a phase of the fcc solid substitutional solution based on copper was formed, and, according to the estimated values, the solubility of cobalt is either close to the boundary or exceeds the maximum solubility according to the equilibrium phase diagram at a temperature of about 1000 °C [4]. The supersaturated solid solution obtained by cryo-HPT is characterized by a higher proportion of deformationally dissolved cobalt than the solution after room HPT. Considering that such a state is characterized by less dispersion, lattice strains and anisotropy of crystallite sizes, we can say that between the cryo-HPT process and studying with

synchrotron radiation, i.e. at room temperature, a post dynamic recrystallization began. In this case, no decay of supersaturated solid solution was noted.

TABLE 3. Estimated values of the lattice parameter (a), Co fraction of Au-Co solid solution, average coherent scattering region size (D), lattice strain (ε) in the center and at the periphery of alloy samples after room- and cryo-HPT.

P, GPa	e	Temperature Mode of Deformation	Sample Region of Studying	a, nm	Au-X at. % Co	D, nm	ε * 10-2 , arb. units	Texture Severity
8	8,1	RT	Center	0,3985±0,0004	25±1	2,2	3,6	strong
			Periphery	0,3982±0,0001	26,5±0,5	2,0	4,0	greatest
		LN	Center	0,3949±0,0005	34±1	3,2	2,6	weak
			Periphery	0,3914	40	-	-	weak

ACKNOWLEDGMENTS

The work was done at the shared research center SSTRC on the basis of the VEPP-4 - VEPP-2000 complex at BINP SB RAS, using equipment supported by project RFMEFI62119X0022.

The SR XRD performed at the station "Diffractometry in the "hard" X-ray range" of the 4th synchrotron radiation channel of the VEPP-3 accelerator of the Siberian Center of Synchrotron and Terahertz Radiation of the Budker Institute of Nuclear Physics by Alexey I. Ancharov.

Obtaining and deformation processing of the investigated materials were carried out on the basis of M.N. Mikheev Institute of Metal Physics of the Ural Branch of the Russian Academy of Sciences, Yekaterinburg.

The research was carried out within the state assignment of Ministry of Science and Higher Education of the Russian Federation (theme “Pressure” No. AAAA-A18-118020190104-3), supported in part by RFBR (project No. 19-32-60039).

REFERENCES

1. A. E. Berkowitz, J. R. Mitchell, M. J. Carey, A. P. Young, D. Rao, A. Starr, S. Zhang, F. E. Spada, F. T. Parker, A. Hutten and G. Thomas, J. of Appl. Phys. **73**, 5320–5325 (1993).
2. S. Liu, J. Jie, Z. Guo, S. Yue and T. Li, Mater. Chem. Phys. **238**, 121909 (2019).
3. A. Bachmaier, G. Rathmayr, J. Schmauch, N. Schell, A. Stark, N. De Jonge and R. Pippan, J. Mater. Res. **34**, 58–68 (2019).
4. H. Okamoto, T. B. Massalski, M. Hasebe and T. Nishizawa, Bull. Alloy Phase Diagrams **6**, 449–454 (1985).
5. A. R. Miedema, P. F. de Chatel, and F. R. de Boer, Physica B+C **100**, 1–28 (1980).
6. M. Monev, R. Bretzler, D. Tatchev and A. Zielonka, Int. J. Surf. Sci. Eng. **95**, 255-260 (2017).
7. G. Zibold and D. Korn, Physica B+C **107**, 99-100 (1981).
8. C. Maurizio, V. Mattarello, B. Kalinic, N. Michieli, I. G. Balasa, C. Scian and G. Mattei, Surf. Coat. Tech. **385**, 125309 (2020).
9. D. Luo, T. Huminiuc, Y. Huang, T. Polcar and T.G. Langdon, Mat. Sci. Eng. A **790**, 139693 (2020).
10. W. Bednarczyk, J. Kawałko, M. Wątroba, N. Gao, M. J. Starink, P. Bała and T. G. Langdon, Mat. Sci. Eng. A **776**, 139047 (2020).
11. R. V. Sundeev, A. V. Shalimova, N. N. Sitnikov, O. P. Chernogorova, A. M. Glezer, M. Y. Presnyakov, I. A. Karateev, E. A. Pechina, A. V. Shelyakov, J. Alloys Compounds **845**, 156273 (2020).
12. A. I. Ancharov, Bull. Russ. Acad. Sci. Phys. **79**, 26–30 (2015).
13. A. I. Ancharov, Russ Phys J **60**, 543–549 (2017).
14. P. A. Piminov G. N. Baranov A. V. Bogomyagkov D. E. Berkaev V. M. Borin V. L. Dorokhov S. E. Karnaev V. A. Kiselev E. B. Levichev O. I. Meshkov S. I. Mishnev S. A. Nikitin I. B. Nikolaev S. V. Sinyatkin P. D. Vobly K. V. Zolotarev and A. N. Zhuravlev, Phys. Procedia **84**, 19-26 (2016).
15. O. A. Kuts, S. V. Starenchenko, Y. V. Solov’eva, V. A. Starenchenko, V. P. Pilyugin and A. I. Ancharov, Optoelectron.Instrument.Proc. **55**, 133–137 (2019).
16. Y. V. Solov’eva, S. V. Starenchenko, V. A. Starenchenko and A. I. Ancharov, J. Synch. Investig. **14**, 158–162 (2020).

17. M. V. Degtyarev, T. I. Chashchukhina, L. M. Voronova, A. M. Patselov and V. P. Pilyugin, Acta Mater. **55**, 6039–6050 (2007).